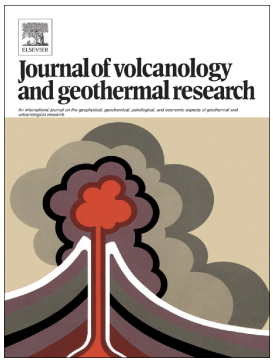

The buried caldera boundary of the Vesuvius 1631 eruption revealed by present-day soil CO2 concentration

M. Poret, A. Finizola, T. Ricci, G.P. Ricciardi, N. Linde, G. Mauri, S. Barde-Cabusson, X. Guichet, L. Baron, A. Shakas, M. Gouhier, G. Levieux, J. Morin, E. Roulleau, F. Sortino, R. Vassallo, M.A. Di Vito, G. Orsi

PII: S0377-0273(18)30346-9
DOI: https://doi.org/10.1016/j.jvolgeores.2019.01.029
Reference: VOLGEO 6552

To appear in: *Journal of Volcanology and Geothermal Research*

Received date: 15 August 2018
Revised date: 16 January 2019
Accepted date: 17 January 2019

Please cite this article as: M. Poret, A. Finizola, T. Ricci, et al., The buried caldera boundary of the Vesuvius 1631 eruption revealed by present-day soil CO2 concentration, Journal of Volcanology and Geothermal Research, https://doi.org/10.1016/j.jvolgeores.2019.01.029

The buried caldera boundary of the Vesuvius 1631 eruption revealed by present-day soil CO_2 concentration

M. Poret [a], A. Finizola [b], T. Ricci [c], G.P. Ricciardi [d], N. Linde [e], G. Mauri [f], S. Barde-Cabusson [g], X. Guichet [h], L. Baron [e], A. Shakas [e], M. Gouhier [g], G. Levieux [i], J. Morin [g], E. Roulleau [g], F. Sortino [j], R. Vassallo [k], M.A. Di Vito [d], G. Orsi [l]

[a] Istituto Nazionale di Geofisica e Vulcanologia, Bologna, Italy

[b] Laboratoire GéoSciences Réunion, Université de La Réunion, Institut de Physique du Globe de Paris, CNRS, UMR 7154, Sorbonne Paris Cité, La Réunion, France

[c] Istituto Nazionale di Geofisica e Vulcanologia, Roma, Italy

[d] Istituto Nazionale di Geofisica e Vulcanologia, Osservatorio Vesuviano, Napoli, Italy

[e] Applied and Environmental Geophysics Group, Institute of Earth Sciences, University of Lausanne, Switzerland

[f] Center for Hydrogeology and Geothermics, University of Neuchâtel, Switzerland

[g] Université Clermont Auvergne, CNRS, IRD, OPGC, Laboratoire Magmas et Volcans, Clermont-Ferrand, France

[h] Geosciences Division, IFP Energies nouvelles, Rueil-Malmaison, France

[i] Ministère chargé de l'environnement, Paris, France

[j] Istituto Nazionale di Geofisica e Vulcanologia, Palermo, Italy

[k] Université Savoie Mont Blanc, Université Grenoble Alpes, CNRS, IRD, IFSTTAR, ISTerre, Grenoble, France

[l] Dipartimento di Scienze della Terra, dell'Ambiente e delle Risorse, Università Federico II, Napoli, Italy

Abstract

Volcanic risk at Vesuvius is one of the highest in the world due to the ~670,000 inhabitants living in the Red Zone, the area exposed to both pyroclastic flows and tephra fallout, to be evacuated before renewal of any eruptive activity. The national emergency plan for Vesuvius builds its risk zonation on a scenario similar to the last sub-Plinian eruption, which occurred in 1631. This study aims at providing new insights on the geometry of the caldera associated with this historical eruption. The impact of past Vesuvius eruptions on present-day soil CO_2 concentration has been investigated by means of an extended geochemical survey carried out for identifying the circulation pathways of hydrothermal fluids inside the volcano. We performed 4,018 soil CO_2 concentration measurements over the whole Somma-Vesuvius volcanic complex, covering an area of 50 km^2. Besides relatively low values, the results show a significant spatial CO_2 concentration heterogeneity over Somma-Vesuvius ranging from the atmospheric value (~400 ppm) up to

~24,140 ppm. The summit of Vesuvius shows an area with anomalous CO_2 concentrations well matching the crater rim of the 1906 eruption. Along the cone flanks, secondary CO_2 anomalies highlight a roughly circular preferential pathway detected along 8 radial profiles at distances between ~840 m and ~1,150 m from the bottom of the present-day crater resulting from the last eruption in 1944. In depth review of the available literature highlights an agreement between this circle-like shaped anomaly and the 1631 sub-Plinian eruption caldera boundary. Indeed, based on the historical chronicles the depression produced by the 1631 eruption had a diameter of 1,686 m, whereas the CO_2 circular anomaly indicates a diameter of 1,956 m. Finally, the results were compared with a 3-D density model obtained from a recent gravity survey that corroborates both the literature and the CO_2 data in terms of potential buried structure at the base of the Vesuvius cone.

Keywords: Somma-Vesuvius, soil CO_2 concentration, 1631 sub-Plinian eruption, carbon dioxide, caldera.

1. Introduction

Carbon dioxide (CO_2) is the second most abundant volatile dissolved in magma after water, and starts exsolving at several kilometres depth due to its low solubility in silicate melts (Gerlach, 1986). CO_2 rises up to the surface through permeable zones, which may also drain other fluids such as hot steam. In fact, spatial correlations between soil gas and thermal anomalies suggest the existence of permeable pathways (e.g. faults and fractures) through which heat and mass transfer towards the surface (Chiodini et al., 2001a; Cardellini et al., 2003; Finizola et al., 2003; 2006; Lewicki et al., 2003; Brothelande et al., 2014).

Previous studies on volcanoes showed that extended soil CO_2 gas surveys allow to defining the main diffuse degassing structures representing structural planes of higher permeability (Barberi and Carapezza, 1994; Chiodini et al., 2001a; Finizola et al., 2002; Cardellini et al., 2003; Lewicki et al., 2003; Granieri et al., 2006; Barde-Cabusson et al., 2009; Carapezza et al., 2009; Schütze et al., 2012). In particular, Chiodini et al. (2001a) was the first to define “diffuse degassing structure” (DDS) and where a specific structural survey was performed to investigate the relations between diffuse degassing and the patterns of fractures and faults. Then, Cardellini et al. (2003), quantified the concept of DDS. A soil gas survey permits quantifying the total soil diffuse degassing and its

evolution with time, as well as defining structures (e.g. caldera borders, fractures, faults; Etiope et al., 1999; Finizola et al., 2002). Diverse techniques such as the dynamic CO_2 concentration method (Camarda et al., 2006) and the soil diffuse degassing method (Farrar et al., 1995; Chiodini et al., 1998; Granieri et al., 2013) can be used in soil CO_2 gas survey. It is worth noting that the soil CO_2 concentration method is not a direct measurement of soil CO_2 degassing and is limited being affected also by soil permeability. One of the critical problems in dealing with this method is the identification of the anomaly sources; in particular those related to deep or organic surface origins. In several cases, this issue can be overcome due to the significant highest concentration (more than one order of magnitude) of the deep-origin anomalies related to magma degassing with respect to the shallow organic contribution. Probabilistic approaches (Sinclair, 1974) are also used to define the threshold between the different populations of the CO_2 anomalies (e.g. Chiodini et al., 1998; 2001a). The application of the soil CO_2 concentration method has yielded good results on volcanoes characterised by 1) a permanent mild explosive activity (Stromboli – Finizola et al., 2002, 2003, 2006, 2009; Revil et al., 2004, 2011; and Yasur volcanoes – Brothelande et al., 2016), or 2) an intense degassing activity and close conduit (La Fossa of Vulcano – Revil et al., 2008; Barde-Cabusson et al., 2009; and La Soufrière de la Guadeloupe – Allard et al., 1998; Brothelande et al., 2014).

The identification of structural limits (i.e. permeable zones) and their subsequent monitoring play a fundamental role in the timely detection of likely precursors of a volcanic eruption (e.g. increase of gas emission) and its related hazard assessment. In case of unrest, gas flow increase along permeable zones can be related to (i) the increase in permeability due to seismic activity and pressurization, (ii) deformation processes or (iii) the increase in magma degassing. Despite the theoretical causes behind diffuse degassing, its monitoring is of the highest importance to understand processes involved in gas emission on active volcanoes.

The recognition of zones characterized by high permeability requires a high spatial resolution (i.e. spacing measurement from meters to few tens of meters). Several studies have permitted to identify the main active structural boundaries dragging magmatic and hydrothermal fluids towards the surface (Finizola et al., 2002; 2003; Lewicki et al., 2003; Granieri et al., 2006; Carapezza et al., 2009; Mauri et al., 2012).

As in other dormant volcanoes, Vesuvius, a high-risk volcano in the densely inhabited Neapolitan area, is affected by diffuse degassing as shown by several studies (Aiuppa et al., 2004; Frondini et al., 2004; Granieri et al., 2013). These studies were based on surveys performed by means of diffuse degassing techniques; namely through the soil diffuse CO_2 flux (accumulation chamber method, Frondini et al., 2004; Granieri et al., 2013) and the soil CO_2 concentration (Aiuppa et al., 2004). The two studies based on the soil CO_2 flux aimed at quantifying the total diffuse degassing of the Vesuvius cone through randomly but homogeneously distributed measurements over the whole area, and identifying the main DDS. The latter aim was also pursued by Aiuppa et al. (2004).

The present study aims at identifying the DDS of the Vesuvius cone through the use, for practical reasons, of the soil CO_2 concentration method, as in Aiuppa et al. (2004), but at higher resolution (shorter measurement spacing and higher density of measurements). This study reports the results from several extensive field campaigns carried out over the entire Somma-Vesuvius volcanic complex. The relatively low degassing activity at Vesuvius and the presence of areas covered by dense forests could limit the identification of anomalies related to structural limits (i.e. faults and fractures), as magma degassing and superficial organic respiration might yield similar CO_2 contributions. For this reason, throughout the fieldworks we strategically opted for a short spacing (20 m) between measurements to reveal anomaly widths, and thereby, to distinguish signal caused by structural elements from those of superficial organic origin. Indeed, several works (e.g. Finizola et al., 2002; Brothelande et al., 2014) have evidenced structural elements (i.e. crater and caldera boundaries or faults) characterizing low width CO_2 concentration anomalies (40-200 m). Results from the CO_2 measurements are compared with the historical literature related to the 1631 sub-Plinian eruption, and also with the results of recent gravity measurements performed over the whole edifice, for better understanding the origin and the present-day role of the main structural boundaries acting as preferential pathways for fluids inside the Vesuvius cone.

2. Geological and structural settings

The Somma-Vesuvius volcanic complex (Fig. 1) is a stratovolcano made of a multistage caldera, Mt. Somma, and a nested younger volcano, Vesuvius. Its volcanism (i.e. from ~373 ka BP) is related to the subduction of the Adriatic-Ionian lithosphere below the Tyrrhenian basin (Fig. 1a).

During its eruptive activity, Mt. Somma has been partially dismantled by caldera collapses related to four Plinian eruptions, which occurred in 22,030 ± 175 (Pomici di Base), 8,890 ± 90 (Mercato), and 3,945 ± 10 yr cal BP (Avellino), and the Pompei eruption in A.D. 79 (Bertagnini et al., 1998; Cioni et al., 1999; Andronico and Cioni, 2002; Santacroce and Sbrana, 2003; Santacroce et al., 2008). The Vesuvius cone has grown within this multistage caldera (hereinafter Mt. Somma caldera) and has produced its last eruption in 1944 (Santacroce et al., 2008). At Vesuvius, periods of close conduit rest were usually interrupted by sub-Plinian eruptions. Two large explosive events disrupted the growth of the cone after A.D. 79: the Pollena (A.D. 472; Rosi and Santacroce, 1983; Mastrolorenzo et al., 2002; Rolandi et al., 2004; Sulpizio et al., 2005), and the 1631 sub-Plinian eruptions (Arnò et al., 1987; Rosi et al., 1993). The last eruptive open conduit period of Vesuvius, characterised by lava effusions and mixed effusive-explosive episodes, began after the 1631 eruption and lasted more than three centuries (Cioni et al., 2008) ending with the 1944 eruption. In particular, the 1794, 1822, 1872, and 1906 eruptions were the most intense events (VEI 2–3). All of them started with lava effusions followed by rapid transitions towards magmatic explosions with lava fountains, sustained columns, and occasionally by phreatomagmatic explosions (Santacroce, 1987; Santacroce et al., 1993; Marianelli et al., 1999; Arrighi et al., 2001). Since 1944, Vesuvius is characterized by low energy seismicity beneath the cone (e.g. max M3.6 on October 1999 and below M3 since 2000). Since 1944, temperature of fumarolic emissions in the summit area has decreased from typical magmatic values (more than 500°C until the beginning of 1960), down to typical shallow hydrothermal steady state temperature, with water boiling temperature at that altitude, ~95°C since the period 1995-2000 (Chiodini et al., 2001b; Del Pezzo et al., 2013).

From a tectonic point of view, Somma-Vesuvius is located at the intersection of two main northwest-southeast and northeast-southwest oriented regional fault systems (Fig. 1b; Ippolito et al., 1973; Pescatore and Sgrosso, 1973; Acocella and Funiciello, 2006; Principe et al., 2010). These two directions have been retrieved also from statistical analysis of fault planes at the scale of the edifice (Bianco et al., 1998), and from the eruptive fissures affecting the volcano flanks (Tadini et al., 2017) and the dykes cutting the Somma caldera walls (Marinoni, 1995). They have also been highlighted by large-scale seismic and gravity data, locating Somma-Vesuvius over a major northeast-southwest structure (Acocella and Funiciello, 2006, and references therein). Additionally, some vents along the Mt. Somma flanks tend to align along this fault system (Ventura and Vilardo, 2006; Tadini et al., 2017).

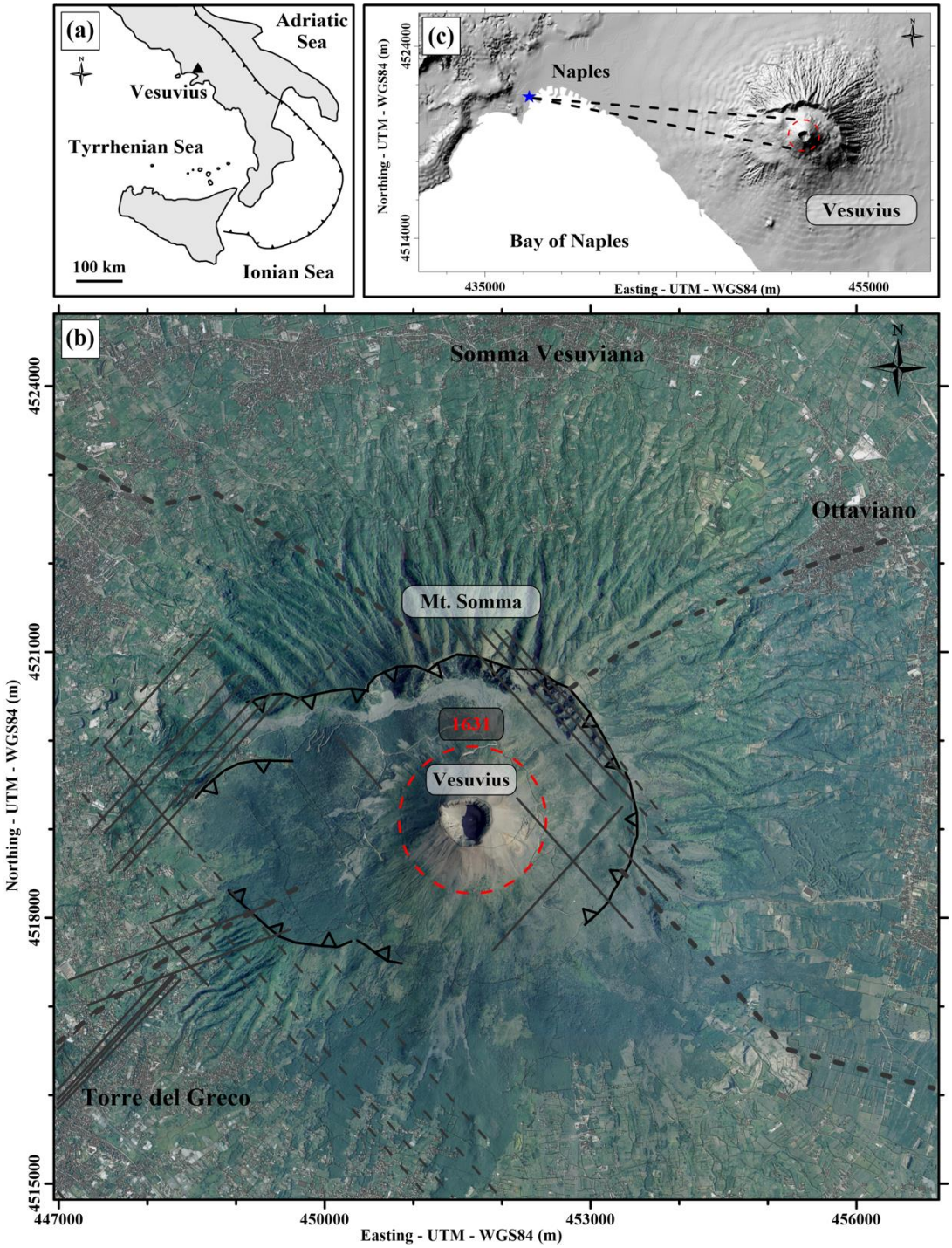

Figure 1: a) Location of the Somma-Vesuvius volcanic complex (Italy) in the subduction context. b) DEM of the Somma-Vesuvius volcanic complex (Vilardo et al., 2008) with the Mt. Somma caldera boundary (Cioni et al., 1999). The regional faults (thick dashed lines), the main faults (dashed lines) and the fractures (solid lines) are from Principe et al. (2010). The red circle refers to the 1631 caldera limit measured by Carafa (1632). c) Map of the bay of Naples with the location of "*Palazzo Reale*" (blue star), from which Carafa (1632) painted and described the Vesuvius 1631 eruption (Fig. 2a). The black dashed lines highlight the relative view of the Vesuvius descriptions. The red dashed circle as in inset b.

The present-day Mt. Somma caldera boundary shows a substantial difference between its northern and southern sectors (Fig. 1b). In particular, the northern sector is less exposed to lava flows than the southern one. Indeed, the northern sector is almost fully covered by organic soil and vegetation, whereas the southern part is mostly covered by post A.D. 79 tephra deposits and lava flows (Ventura et al., 1999).

Present-day Vesuvius crater rim (hereinafter 1944 crater rim; Fig. 1b) shows a sharp asymmetric topographic profile, which corresponds to the intersection between lava-fill of the crater left by the 1906 eruption and the crater produced by the 1944 eruption, whose edge lies southwest from the 1906 crater (Fig. 1b). This intersection is a preferential path for deep gas rising upwards and affecting the Vesuvius edifice (Frondini et al., 2004; Granieri et al., 2013). In addition, this intersection also separates the southwest crater area from the rest of the crater highlighting an elevation discrepancy (i.e. ~120 m) in favour of the northeast sector of Vesuvius, which features the summit at 1,281 m above sea level (a.s.l.).

3.1. The 1631 sub-Plinian eruption

In 1631, a sub-Plinian eruption affected the structural setting of Vesuvius inducing a caldera collapse (e.g. Braccini, 1631; 1632; Carafa, 1632; Masculo, 1633; Nazzaro, 1989). Carafa's report (1632) contains a detailed reconstruction of the event. In particular, the authors mentioned that before the 1631 eruption, the Vesuvius summit was ~55 m higher than Mt. Somma, with a crater of ~1,500 m and ~480 m in circumference and diameter, respectively. These dimensions increased respectively to ~5,230 m and ~1,690 m after the eruption. The scheme of such observations is reported in the painting displayed in Fig. 2a, showing the outline of the Somma-Vesuvius shape, while Fig. 2b reveals the impact of the 1631 eruption on the Vesuvius morphology. It is worth noting that the right and left insets in Fig. 2b are respectively paintings of the Somma-Vesuvius prior and during the 1631 eruption. In addition to the above morphological aspects, the location where the observations were done can be inverted through the paintings (Figs. 2a and 2b), which is more likely to be the *Palazzo Reale* in the city of Naples (blue star in Fig. 1c).

According to the chronicle summary compiled by Rosi et al. (1993), the 1631 eruption was characterized by four phases. It began with an opening phase in the early morning of 16 December

after a sequence of strong earthquakes. An eruptive fissure opened and extended from the top to the base of the cone along the western flank (also visible on the paintings in Figs. 2a and 2b).

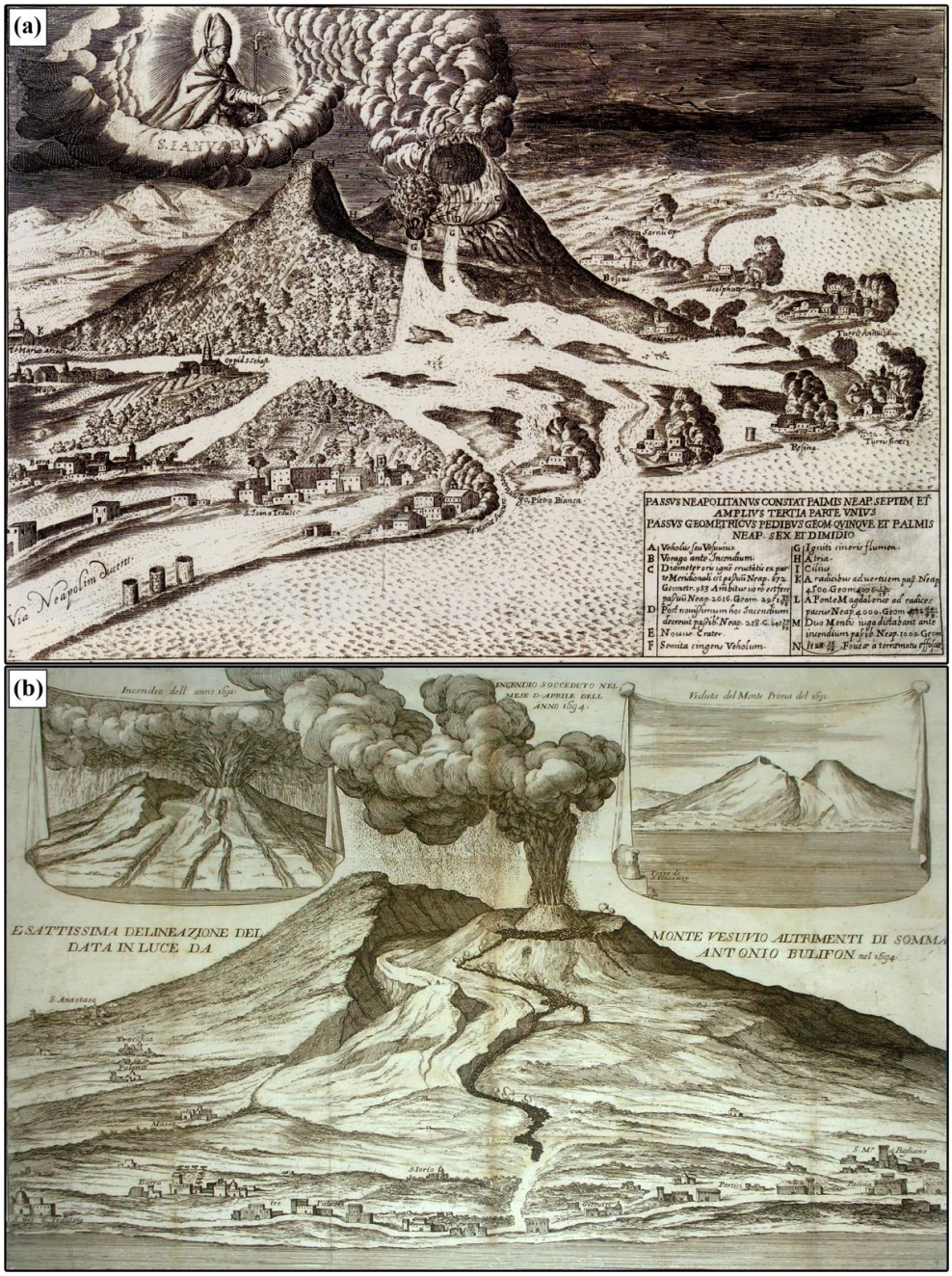

Figure 2: a) Painting from "*Palazzo Reale*" (see Fig. 1c) of Somma-Vesuvius after the 1631 eruption (Carafa, 1632). The letters refer to Carafa's measurements for characterizing the 1631 caldera (legend in the lower right). b) Painting of Somma-Vesuvius showing the 1694 eruption (Bulifon, 1694) and the 1631 caldera partially filled at the time of the painting highlighting the impact of the 1631 eruption on the Vesuvius cone. The two insets represent the Vesuvius morphology prior (right) and during (left) the 1631 eruption.

In a short time, ash and bombs were reported to fall on the rim of Mt. Somma (Anonymous, 1631a; 1631b). Then, a plume with a spectacular pine-like shape was generated at the base of the eruptive fissure (Masculo, 1633), which then spread out south-eastwards as volcanic ash clouds (Capece, 1631; Anonymous, 1632; Bove, 1632; Masino di Calvello, 1632; Rocco, 1632) up to Greece and Turkey (Constantinople), where ash fallout was reported (Giuliani, 1632).

On 17 December 1631, the subsequent phase of activity was accompanied by seismic shocks and ash fallout in the Neapolitan area. First, a 5-minutes earthquake occurred, which accompanied the collapse of the caldera. From Naples, the collapse was seen as a swallowing of the cone (Rosi et al., 1993). Besides these observations, Carafa (1632) and Masculo (1633) reported an almost instantaneous destruction of the cone accompanied by a ground deformation dropping the sea level down by 6 m with a corresponding sea retreat reaching 2,000 m followed by a 5-m high tsunami. Such observations were painted by Scipione Compagno (Guidoboni, 2008). Pyroclastic flows started simultaneously with the caldera-forming collapse (Rosi et al., 1993). However, the pyroclastic flows were reported by the eyewitnesses in such a confused manner that for centuries the flows were interpreted as lava flows. The unequivocal emission of pyroclastic flows was first documented by Carracedo et al. (1993) and Rosi et al. (1993). Finally, the eruption ended with a final stage of ash and water vapour emission prior ash fallout and lahars along the slopes of the volcano (Rosi et al., 1993). When emissions of pyroclastic flows stopped, the first observations reported an elevation drop of the new Vesuvius summit below the Mt. Somma top, with caldera dimension clearly greater than the crater before the onset of the eruption (Masino di Calvello, 1632).

Based on sight observations (Guidoboni, 2008), the comparison and integration of field-based physical volcanology data and chronicles (Rosi et al., 1993) with paleomagnetism study on volcanic hazards (e.g. pyroclastic flows; Carracedo et al., 1993) suggest that the 1631 eruption has played a major role on the morphological evolution of the Vesuvius cone.

Being the last major eruption of Vesuvius, the 1631 sub-Plinian eruption was considered in the first national emergency plan, edited by the Italian Civil Protection Department, as the “maximum expected event” and reference scenario in case of renewal of the activity in the short- or mid-term (Barberi et al., 1995; DPC, 1995; Ricci et al., 2013). The current reference scenario for the updated plan (DPC, 2015) is still a sub-Plinian event similar to that of 1631. The area immediately

surrounding the volcano, named Red Zone, is prone to volcanic hazards related to flowage of pyroclastic density currents and lahars, and tephra fallout (Tadini et al., 2017). It includes 25 municipalities with ~670,000 inhabitants, which must be evacuated before the onset of the next eruption (DPC, 2015).

3.2. Observations from literature

In terms of morphological observations of the 1631 eruption, a critical review of the available literature highlights significant differences relative to the circumference (C) and diameter (D) of the crater produced by the eruption (e.g. Rosi et al., 1993). The two insets on Fig. 2b represent the Vesuvius morphology prior (right) and during (left) the 1631 eruption, while the main painting of Fig. 2b highlights the 1631 caldera partially filled at the time of the painting (1694 eruption; Bulifon, 1694). Table 1 summarizes the estimates of D from several authors, which ranges from ~1,682 to 2,949 m. It is worth noting that the measurements were made by means of non-universal measurement units (e.g. *Passo Napoletano – PN* and *Miglio Italiano – MI*), which require to be converted into meters (1.933 and 1,853 m for the *PN* and *MI*, respectively). Although most of the authors assessed C only (Table 1), Carafa (1632) and Masculo (1633) measured both C and D. It follows that for the cases where only C is provided, we estimated D by means of the relationship between C and D.

The available estimates of the 1631 caldera diameter are displayed in Fig. 3. With the exception of the measurement performed by Braccini (1632; label 2 in Fig. 3), diameter measurements indicate a nearly linear evolution with time of the caldera dimension, showing an increase of more than 1,000 m in 100 years. This can be likely ascribed to the morpho-structural evolution of the high-angle and intensely fractured caldera wall (i.e. caldera wall collapses). Despite the difficulty in evaluating the data accuracy provided by the authors, those of Braccini have not been used for defining the regression line in Fig. 3, and were considered not reliable. Accordingly to the detailed description of the 1631 eruption features, also consistent with the reconstruction of Rosi et al. (1993), the data provided by Carafa (1632; label 1 in Fig. 3) have been taken as reference for performing a comparative analysis with the results of this investigation.

	Diameter (D)			Circumference (C)			
Year	**Value**	**Unit**	**Value in m**	**Value**	**Unit**	**Value in m**	**References**
1632	**872**	***PN***	**1,686**	**2,703**	***PN***	**5,225**	**Carafa, 1632 [1]**
1632	**—**	**—**	**2,359 ***	**4**	***MI***	**7,412**	**Braccini, 1631, 1632 [2]**
1633	**870**	***PN***	**1,682**	**2,730**	***PN***	**5,277**	**Masculo, 1633 [3]**
1644	**—**	***PN***	**1,769 ***	**3**	***MI***	**5,559**	**Evelyn, 1644 [4]**
1648	**—**	**—**	**1,769 ***	**3**	***MI***	**5,559**	**Raymond, 1648 [5]**
1663	**—**	***PN***	**1,769 ***	**3**	***MI***	**5,559**	**Magalotti, 1779 [6]**
1685	**—**	***PN***	**2,359 ***	**4**	***MI***	**7,412**	**Burnet, 1699 [7]**
1695	**—**	**—**	**2,359 ***	**4**	***MI***	**7,412**	**Drummond, 1845 [8]**
1734	**—**	***PN***	**2,949 ***	**5**	***MI***	**9,265**	**Sorrentino, 1734 [9]**

Table 1: Diameter (D) and circumference (C) measurements of the 1631 caldera with the corresponding units and conversion in meters. *PN* stands for *Passi Napoletani* unit and *MI* for *Miglio Italiano* unit. * Diameter calculated from direct circumference measurements. Numbers in brackets in the References column refer to Fig. 3.

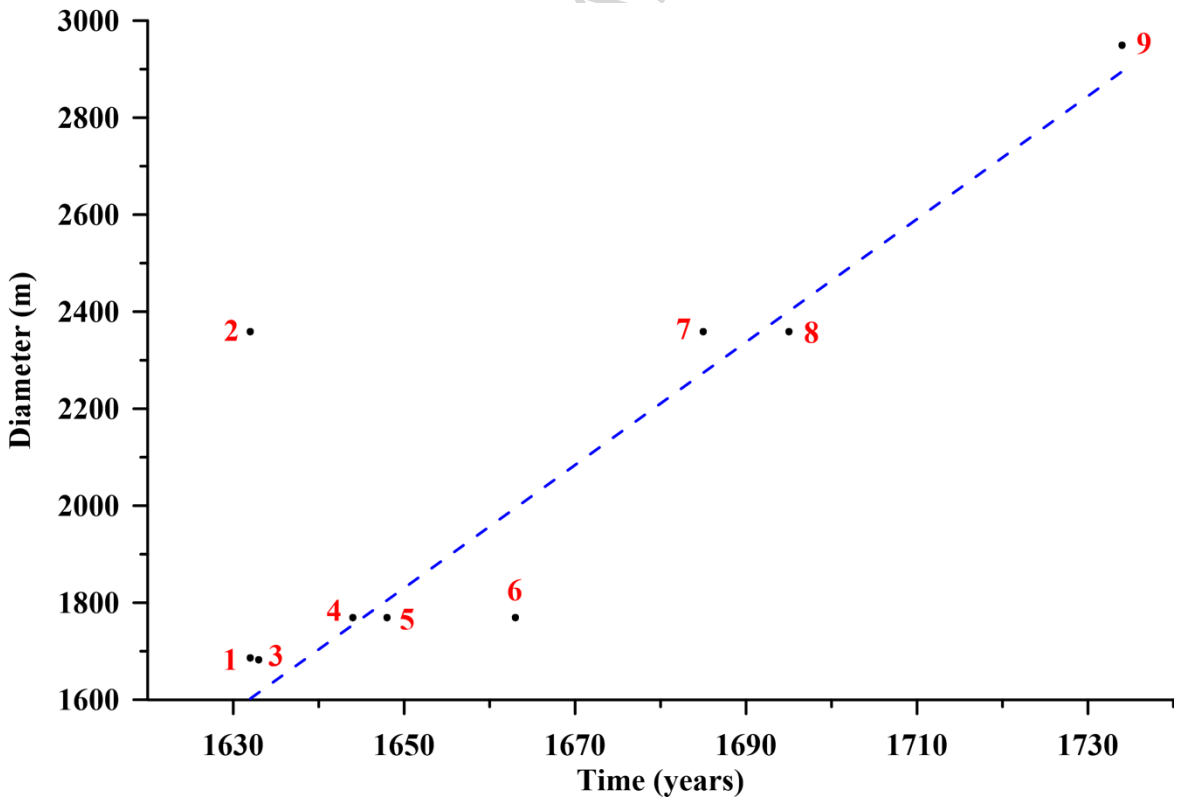

Figure 3: Measurements of the 1631 caldera diameter from literature. The blue dashed line represents the linear regression of diameter measurements, excluding the label 2 (see Sect. 3.1). Red numbers refer to the references presented in Table 1 (see numbers in brackets in the References column).

4. Data acquisition and methodology

A total of 3,949 measurements were carried out during two extensive one-month field campaigns: 1) in July 2001 on the Vesuvius cone (1,668 measurements, 20 m spacing; see Fig. 4a) and 2) in July 2003 in the lowermost part of the edifice including Mt. Somma area and also the profile going down into the actual Vesuvius crater (2,281 measurements, 20 m spacing; see Fig. 4a). A common profile of 98 measurements was carried out along the crater rim both in July 2001 and July 2003 (Fig. 4a). The two datasets were both acquired in July (summer season) to mitigate the effect of external parameters on soil CO_2 concentration, especially those induced by variation of soil moisture. Indeed, soil was relatively dry for all the measurements. In March 2014, a short profile (69 measurements, 20 m spacing) was added to achieved covering the western lower flank of the Vesuvius cone increasing the total amount of measurements up to 4,018. Besides this dataset, during the 2014 campaign, we also acquired a northwest-southeast oriented ~7-km long profile (349 measurements, 20 m spacing; Fig. 4a; Poret et al., 2016). Each measurement was geo-referenced by means of a hand-held GPS. During the two main campaigns, data were collected following eight radial profiles extending from the 1944 crater rim (Fig. 4a) down to the base of the cone (~700 m a.s.l.). For achieving a measurement mesh representative of the entire volcanic complex, we closed the grid by adding three circular profiles 1) along the 1944 crater rim, 2) at the base of the Vesuvius cone, and 3) the largest and topographically lowermost one that includes the Mt. Somma (Fig. 4a).

Soil gas was collected by pumping with a 100 ml syringe through a 3 mm diameter tube inserted at 30 cm depth. CO_2 concentration was measured by injecting the samples into two infrared spectrometers. The high variability of CO_2 concentration, as expected for dormant volcanoes and surrounding areas, motivated the use of two spectrometers. One spectrometer was used to detect and measure low concentrations (< 3000 ppm), while the other is set for higher concentrations (i.e. 3,000–100,000 ppm). The analytical uncertainty related to the CO_2 concentration retrieval is estimated at ± 5% (Finizola et al., 2009).

Considering the uneven distribution of the data (2001 and 2003 campaigns), we produced the CO_2 concentration map by using the Kriging method following two steps, as suggested by Finizola et al. (2002). First, we interpolated through a regional mesh with a resolution of 10-times the sampling

step (i.e. 200×200 m). Then, the resulting interpolation was integrated into the data for locally interpolating at higher resolution (40×40 m). The largest areas with no data were blanked.

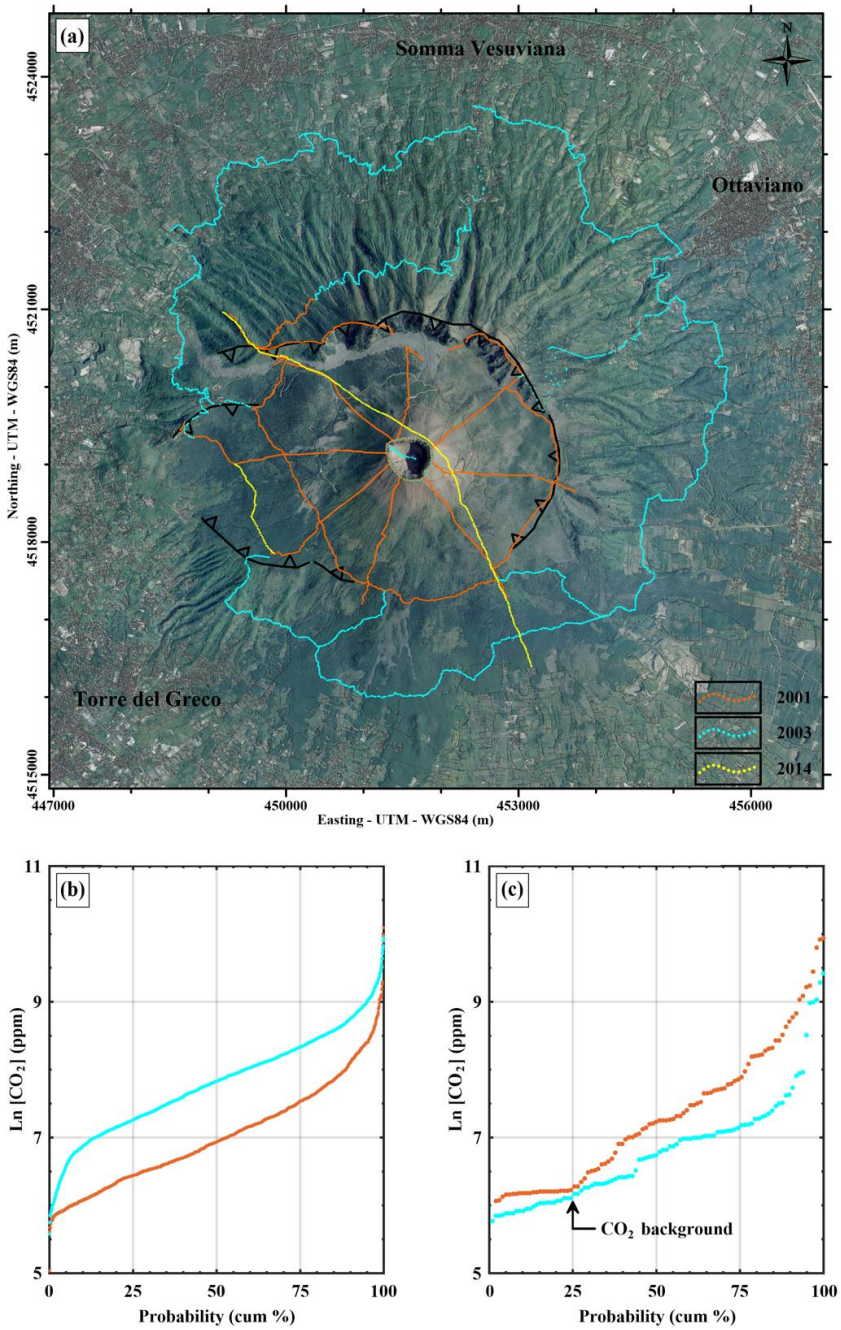

Figure 4: (a) Location of the soil CO_2 concentration measurements performed on July 2001, July 2003 and March 2014 on the Somma-Vesuvius volcanic complex; (b) Probability plot technique (Sinclair, 1974) performed on the 2001 (orange) and 2003 (cyan) soil CO_2 concentration data acquired on the entire volcanic complex; (c) Probability plot technique (Sinclair, 1974) performed on the 2001 (orange) and 2003 (cyan) soil CO_2 concentration data acquired on the reiteration profile located on the crater rim (98 measurements; see Fig. 4a). The CO_2 background of the Somma-Vesuvius volcanic complex, obtained through the probability plot technique, is estimated around 550 ppm.

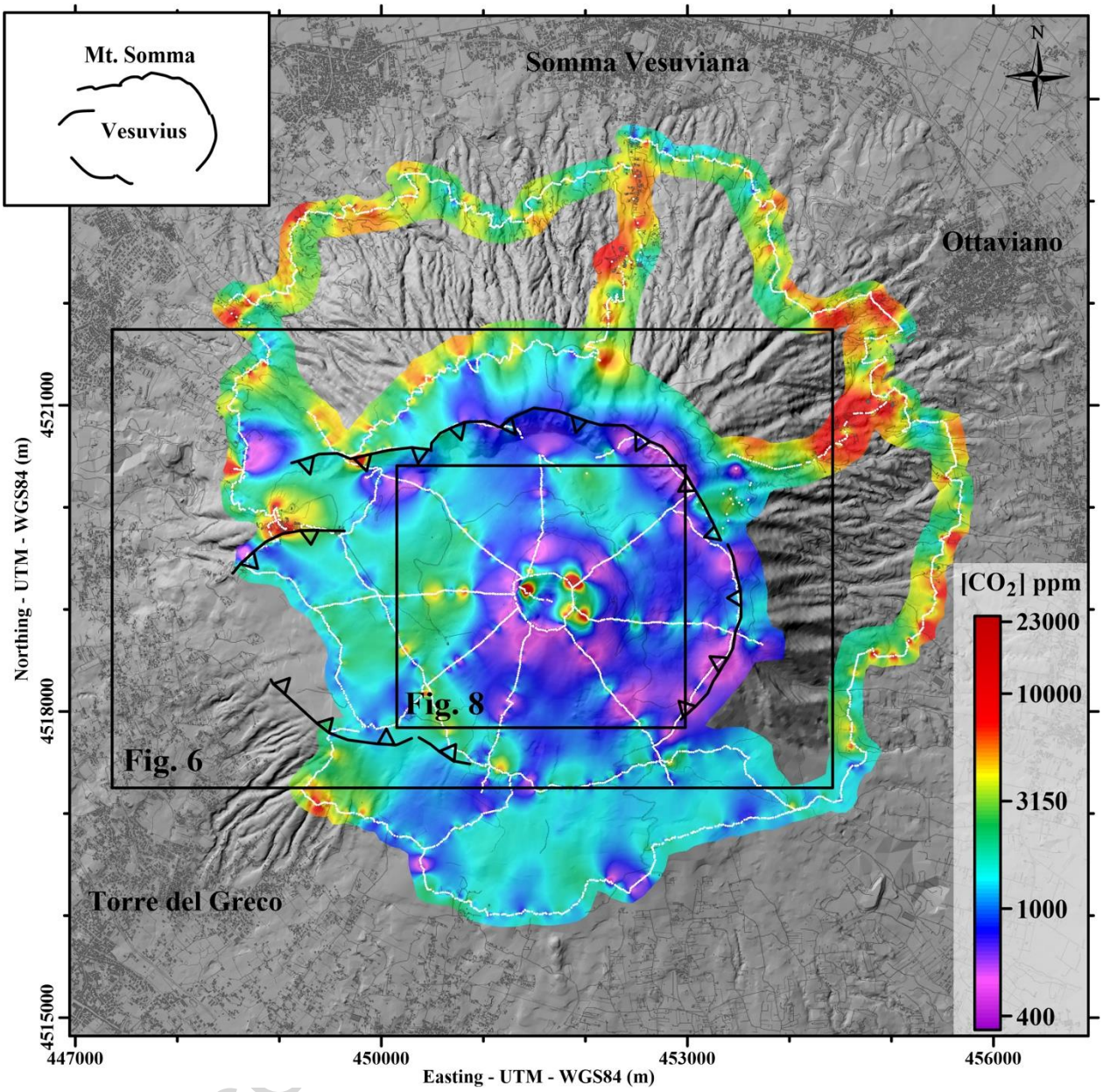

Figure 5: Soil CO_2 concentration map of the Somma-Vesuvius volcanic complex. White dots show the CO_2 measurements. The reported Mt. Somma caldera limit (line with triangles) is extracted from Cioni et al. (1999). The rectangles localize the extension of Figs. 6 and 8.

5. Results and discussion

Before discussing the soil CO_2 concentrations associated with the Somma-Vesuvius volcanic complex, we tested the dataset through the probability plot technique (Sinclair, 1974; Chiodini et al., 1998; 2001a; 2017; Frondini et al., 2004), which can be used for displaying the data and highlighting the different CO_2 populations. First, we considered all the data (2001 and 2003) and the probability plot technique displays values significantly higher in 2003 with respect to 2001 (Fig. 4b). This result is attributed to the locations of the 2003 measurements on the northern flank of Mt. Somma, where dense forests cover investigated area. Then, we also tested the probability plot technique on the 98 CO_2 measurements collected along the 1944 crater rim during both campaigns. The result displays a significant decrease in soil CO_2 concentration between July 2001 and July 2003 (Fig. 4c). As the crater rim is not vegetated, the decrease can be attributed to a slight decrease in magma degassing.

5.1 Soil CO_2 concentration on the Somma-Vesuvius volcanic complex

The soil CO_2 concentrations over the Somma-Vesuvius complex shows relatively low values, ranging between ~400 and ~24,140 ppm (Fig. 5) compared to other active volcanoes. Indeed, La Fossa of Vulcano (Barde-Cabusson et al., 2009), La Soufrière de la Guadeloupe (Allard et al., 1998; Brothelande et al., 2014), and Furnas in the Azores (Viveiros et al., 2010) are characterised by CO_2 concentrations close to 1,000,000 ppm (i.e. 100% in volume).

Figure 5 highlights the areal distribution and the high heterogeneity of the soil CO_2 concentration for the entire Somma-Vesuvius area, from which we can distinguish the following 3 main sectors: 1) the actual summit area of the Vesuvius cone, exhibiting the highest CO_2 concentration values (up to ~24,140 ppm) sometimes associated with sub-fumarolic activity; 2) the flanks of the Vesuvius cone down to the Mt. Somma caldera, characterized by CO_2 background values below 1,000 ppm with scattered CO_2 peaks; 3) the area located outside the Mt. Somma caldera (i.e. N, E, and W flanks), having CO_2 values in average higher (up to 15,000 ppm) than inside the structure. The transition between the last two sectors appears to coincide with the Mt. Somma caldera boundary. However, it is worth noting that this method does not permit distinguishing between CO_2 issued from deep degassing (i.e. volcanic origin) or produced by "soil respiration" (i.e. biogenic origin; Mielnick and Dugas, 2000; Aiuppa et al., 2004). Indeed, by comparing Fig. 5 with

Fig. 1b we observe that sector 3 is dominated by a dense forest being responsible of the abundant presence of CO_2. As a consequence, results obtained from the data collected on the northern slopes of Mt. Somma appear of little significance in the context of volcano-related investigations (i.e. to position buried caldera margins and other structural elements such as faults and fractures). Although less intensive in terms of soil CO_2 concentrations, this is also the case of the bottom of the inner part of the Mt. Somma caldera (i.e. sector 2). In contrast, sector 1 has almost no vegetation but shows localized CO_2 anomalies in the summit area, which are assumed to be related to deep degassing (i.e. volcanic origin; Aiuppa et al., 2004; Frondini et al., 2004).

Taking into consideration the soil CO_2 degassing over the entire volcanic edifice, weak, moderate, and strong degassing areas can be observed, accordingly to other volcanoes (e.g. Galeras, Poas and Rincon de la Vieja – Williams-Jones et al., 2000; Misti – Finizola et al., 2004; Stromboli – Finizola et al., 2002). The weak degassing areas in the upper part of a volcano have been often associated with self-sealing processes induced by hydrothermal activity inside the edifice (e.g. Vulcano, Barde-Cabusson et al., 2009). This interpretation could also be suggested for the Somma-Vesuvius.

5.2 Soil CO_2 concentration on the flanks of the Vesuvius cone

Figure 6 shows that CO_2 anomalies located near the present-day summit area of Vesuvius are well constrained within the 1906 crater boundary, showing significant CO_2 degassing accompanied by low-temperature fumarolic activity. This observation may be related to the location of the main conduit of the 1906 eruption that, during which a peculiar sustained gas jet phase occurred and was described in detail in Perret (1924), and then reported in Bertagnini et al. (1991) and Mastrolorenzo et al. (1993).

It is worth noting that the 8 radial profiles (i.e. N, NE, E, SE, S, SW, W, and NW) tend to have the same CO_2 concentration trend with a peak at ~1 km from the bottom of the 1944 crater (in average 997 m, standard deviation: σ = 103 m). The nearly circular distribution of the CO_2 peaks around the summit area together with the distribution and location of the main volcano-tectonic and regional geological structures (Bianco et al., 1998; Ventura et al., 1999; Principe et al., 2010) as well as the distribution of the eccentric eruptive vents and fractures (Linde et al., 2017 and references therein), lead to assume these anomalies to be independent from the regional volcano-tectonic structures mentioned in Section 2 (Fig. 1b).

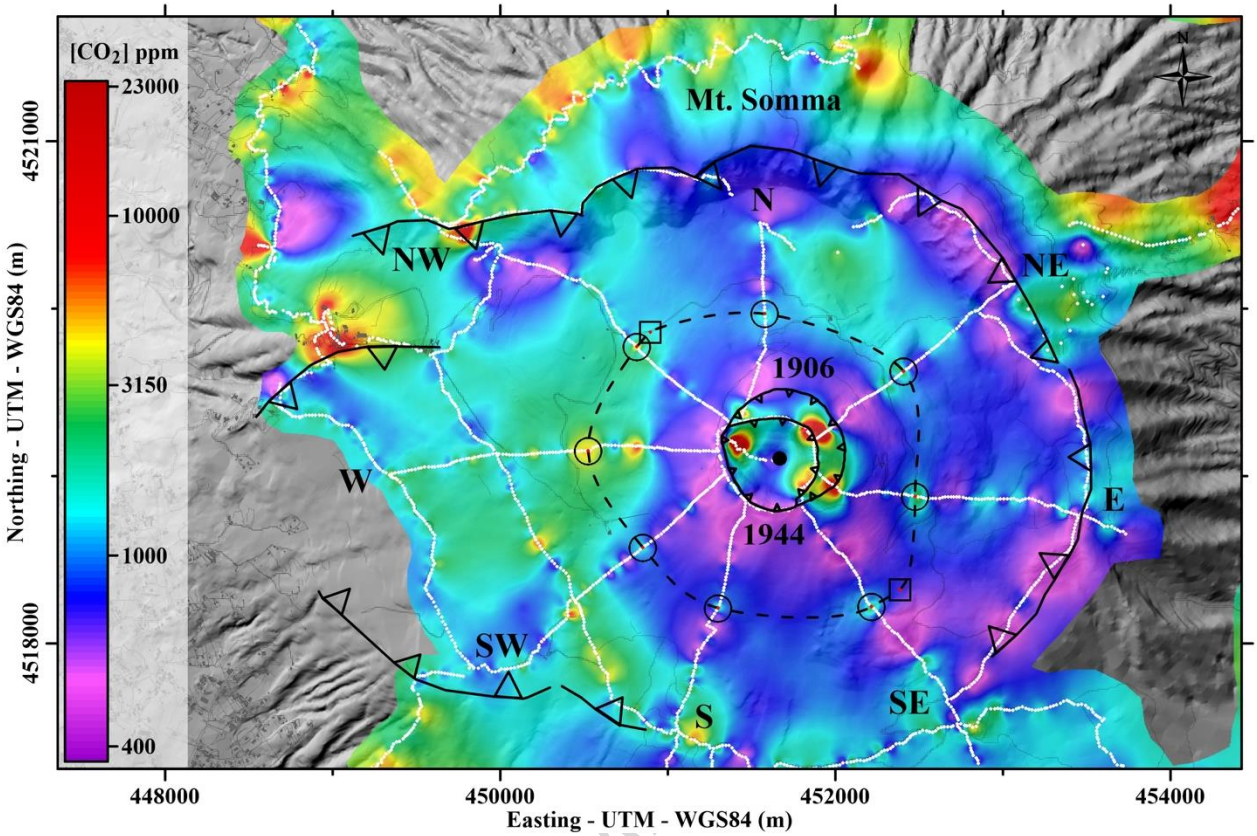

Figure 6: Soil CO_2 concentration map. Circles refer to the CO_2 peaks identified along the 8 radial profiles while squares refer to the NW-SE profile (Poret et al., 2016; details in Table 2). Mt. Somma caldera rim is from Cioni et al., 1999. The 1906 and 1944 crater rims are from Andronico et al., 1995; Santacroce and Sbrana, 2003. Black dot shows the bottom of the 1944 crater.

Comparing the identified CO_2 anomalous peaks (Fig. 6) with the previous studies (Frondini et al., 2004; Granieri et al. 2013), no similar anomalies have been highlighted. Indeed, the measurements of Granieri et al. (2013) are located at higher elevation on the cone than the detected CO_2 anomalous peaks (see Fig. 1a therein), and measurements of Frondini et al. (2004) only partially cover the Vesuvius edifice with higher measurement spacing (i.e. lower spatial resolution than this study; see Fig. 1c therein).

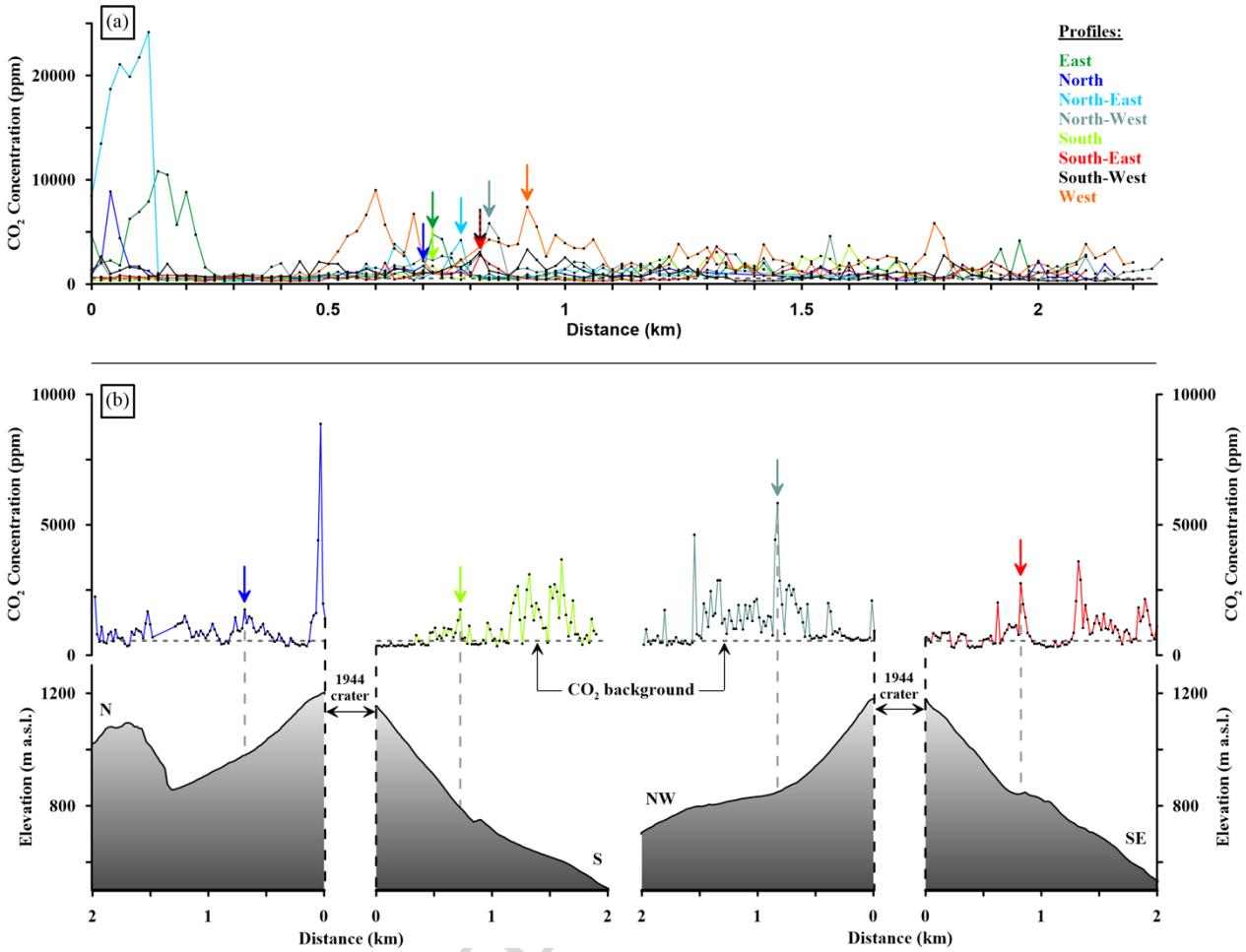

Figure 7: a) Soil CO_2 concentration profiles measured on the Vesuvius cone. Distance is set from the top of the actual crater rim towards the base of the cone. The arrows refer to the CO_2 peaks described in Table 2. The CO_2 background for the Vesuvius cone, 550 ppm, was identified by means of the probability plot method (Sinclair, 1974). b) Example of the N-S and NW-SE CO_2 concentration profiles with the corresponding topography.

In particular, by analysing the 8 profiles from the 1944 crater rim towards the base of the cone shows a systematic local CO_2 increase (arrows in Fig. 7a). The CO_2 concentration peaks range between 1,426 and 7,410 ppm (Table 2). In addition, the same CO_2 anomalies were observed along the NW-SE profile carried out in 2014 (squares in Fig. 6; Table 2; Ricci et al., in prep.), which crossed the entire edifice with a measurement spacing of 20 m (Poret et al., 2016).

Each of the ten radial profiles (i.e. circles and squares in Fig. 6), shows a single CO_2 peak but the W profile, along which two peaks are identified (Figs. 6 and 7a). One peak is located along the western slope of the cone (i.e. 500-700 m from the crater rim), whereas the second is at the base of the cone (i.e. 800-1100 m from the crater rim). Considering the distance between the crater rim and

these two peaks, the one at the base of the cone seems to be likely linked with those of the other profiles. Therefore, only this anomaly located at the base of the cone will be considered for the W profile in this study (Table 2).

Id	Longitude UTM WGS 84	Latitude UTM WGS 84	[CO_2] (ppm)	Altitude (m a.s.l.)	Distance from the 1944 crater rim (m)	Distance from the bottom of 1944 crater (m)
N	**451579**	**4519969**	**1749**	**975**	**675**	**869**
NE	**452406**	**4519627**	**4224**	**933**	**751**	**903**
E	**452475**	**4518878**	**4776**	**950**	**694**	**838**
SE	**452215**	**4518219**	**2766**	**840**	**873**	**1041**
S	**451300**	**4518212**	**1748**	**790**	**735**	**966**
SW	**450851**	**4518573**	**1426**	**791**	**747**	**976**
W	**450524**	**4519150**	**7410**	**797**	**847**	**1146**
NW	**450814**	**4519772**	**5826**	**845**	**790**	**1084**
NW14	**450894**	**4519861**	**2449**	**848**	**804**	**1082**
SE14	**452386**	**4518321**	**2024**	**844**	**827**	**1063**

Table 2: Location of the 10 CO_2 concentration peaks identified on each radial profile with the corresponding CO_2 concentration value, elevation, horizontal distance from the 1944 crater rim, and horizontal distance from the bottom of the 1944 crater.

The circular shape of the observed CO_2 local maxima (Table 2) centred on the 1944 crater (dashed line in Fig. 6), is characterized by the short lateral extension (i.e. ~40–140 m length), and the same order of magnitude for CO_2 concentration (Table 2). Furthermore, the elevation of the CO_2 peaks varies within less than 200 m (from ~790 to ~975 m a.s.l.). The horizontal distance from the 1944 crater rim varies between ~675 and ~873 m, whereas that from the bottom of the 1944 crater between ~838 and ~1,146 m. The rather symmetric shape observed through the CO_2 anomalies indicates an average diameter of ~1,956 m near the base of the Vesuvius cone.

The circular shape from the identified CO_2 peaks (hereinafter "CO_2 limit") suggests the presence of a buried structural feature (dashed line in Fig. 6). On the basis of the historical reports (Carafa, 1632; Rosi et al., 1993), the caldera rim of the 1631 sub-Plinian eruption, with a ~1,686 m diameter (Table 1), appears to be similar to the CO_2 limit. We quantitatively compared the CO_2 limit with

the inferred 1631 caldera boundary (Carafa, 1632), which are both displayed in Fig. 8. Considering the missing information related to the exact location and geometry of the vent in the 1631 eruption, the structural boundary has been centred on the 1944 crater bottom by assuming that the present conduit of Vesuvius remained unchanged since the 1631 eruption, being consistent with Tadini et al. (2017). Furthermore, the location from which the 1631 caldera has been measured (Carafa, 1632; Fig. 1c) implies the assumption of a circular shape geometry. However, as observed on other volcanoes, caldera boundaries are roughly circular but can also present irregularities due to caldera collapse processes and pre-existing structural setting (e.g. Orsi et al., 1999; Roche et al., 2000; Merle and Lénat, 2003; Acocella, 2007; Capuano et al., 2013). The CO_2 limit (Fig. 8) illustrates such an irregular shape, which could not be observed by Carafa (1632) from his viewpoint (Fig. 1c). Considering a non-perfectly circular boundary, the average diameter of the CO_2 limit deriving from the anomalous values is 1,956 m (σ = 129 m), having the largest diameter (~2,125 m) oriented north-west-south-eastwards, and the shortest one (i.e. ~1,834 m) along the north-south profile.

The 1631 caldera boundaries from Carafa (1632) and the CO_2 limit suggested in this study (Fig. 8) coincide in shape, with differences along the radials ranging from 0 (i.e. perfect fit) to ~307 m (in average ~139 m wider than Carafa's measurements). It is worth noting that the comparison between Carafa's measurements and the results of this study for determining the 1631 caldera dimension is only qualitative due to the large uncertainties in both methods. Indeed, by calculating remotely Carafa has assumed a perfect circular shape, observing partially the caldera rim (see Fig. 1c). Furthermore, it is also difficult to assess the degree of accuracy of the painting. Besides, soil CO_2 concentration survey suffers from uncertainties relative to the soil permeability that partially controls the soil CO_2 concentration. Moreover, fracture orientations drive CO_2 towards the surface with a certain angle. Nonetheless, the 1631 sub-Plinian eruption is the last major event at Vesuvius, producing relatively young fractures, potentially having today a greater permeability than the surrounding environment. However, the caldera dimension discrepancies can also reflect the evolution of the caldera walls, with local enlargement of the rim related to landslides affecting the inner and dip caldera slopes.

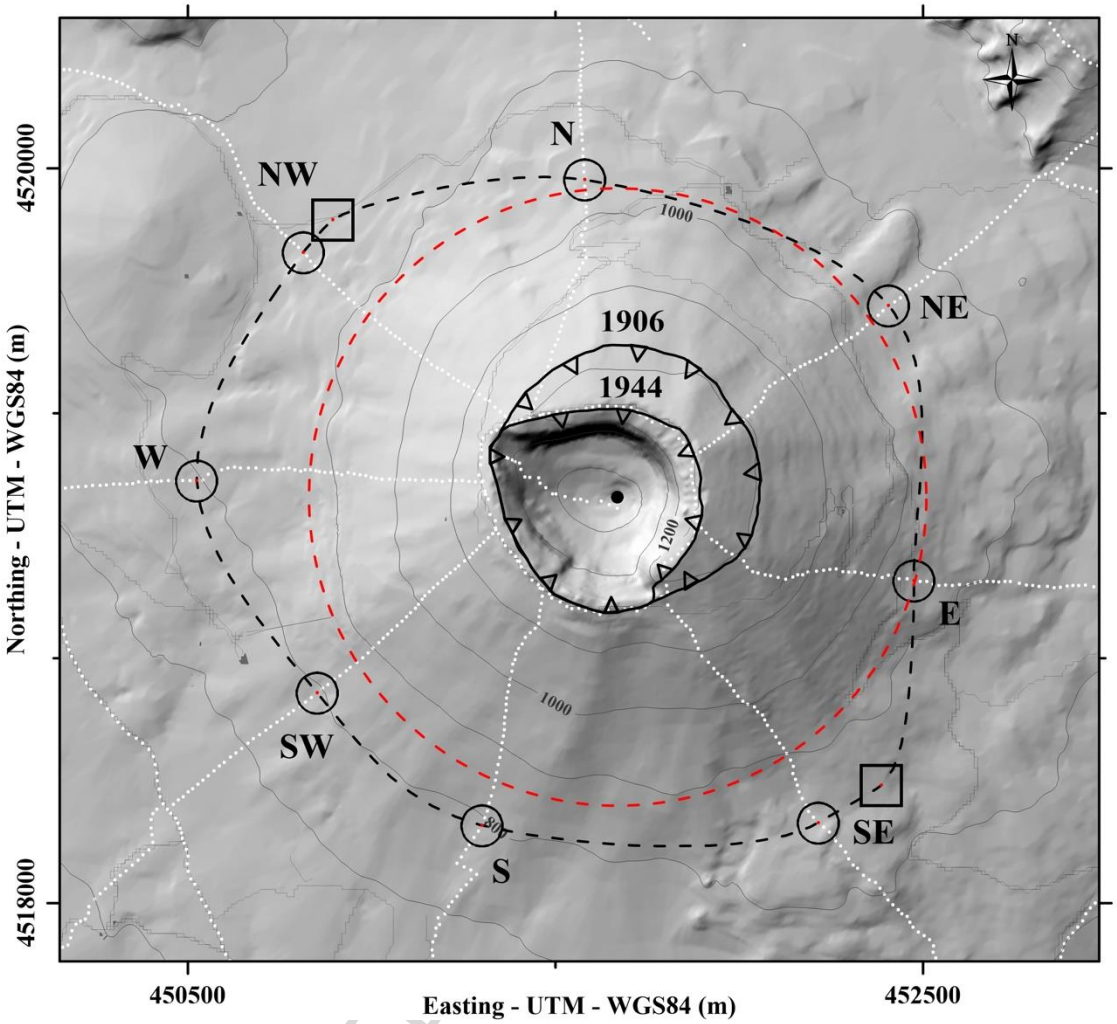

Figure 8: Comparison between the 1631 caldera (Carafa, 1632) and the CO_2 limit. Circles refer to the CO_2 peaks identified along the 8 radial profiles, while squares refer to the NW-SE profile (Poret et al., 2016; see Table 2). Red dashed line is the 1631 caldera boundary (from Carafa, 1632, and Rosi et al., 1993) and the black dashed line is the limit inferred from the CO_2 concentration peaks. Black dot shows the bottom of 1944 crater.

In Fig. 6, the west flank of the Vesuvius cone shows two CO_2 concentration anomalies, reflecting a more complex structure (see also Fig. 7a). To better constrain the effect of the 1631 caldera boundary on the present-day structure of the Vesuvius cone, the CO_2 results were also compared with those of a 3-D density model obtained from a recent gravity survey (Linde et al., 2017). Figure 9 shows the overlapping of the CO_2 limit with two horizontal density slices at 800–900 m and 700–800 m a.s.l. (respectively Figs. 9a and 9b). The two elevation intervals are motivated by the CO_2 peak elevations (Table 2). Indeed, the average elevation of the CO_2 limit is 865 m a.s.l.. The two elevation intervals were therefore chosen for embracing both the average elevation of the supposed 1631 caldera rim as well as its buried structure. The comparison between CO_2 and the density

model highlights the link between the 1631 caldera and the density distribution inside the Vesuvius cone. In addition, Fig. 9 emphasizes a less dense sector (i.e. 2200–2300 kg/m^3) inside the 1631 caldera boundary defined by the CO_2 limit, suggesting that the 1631 caldera was refilled by volcanic products that are less dense than the outer and older part of the Vesuvius cone. These gravimetric results clearly show that the 1631 eruption induced a significant decrease in the global density of the products emitted before and after this major explosive event. Such a lower density distribution is commonly observed on many calderas (e.g. Froger et al., 1998; Brothelande et al., 2016), and strongly supports the hypothesis that the identified CO_2 limit defines the 1631 caldera boundary.

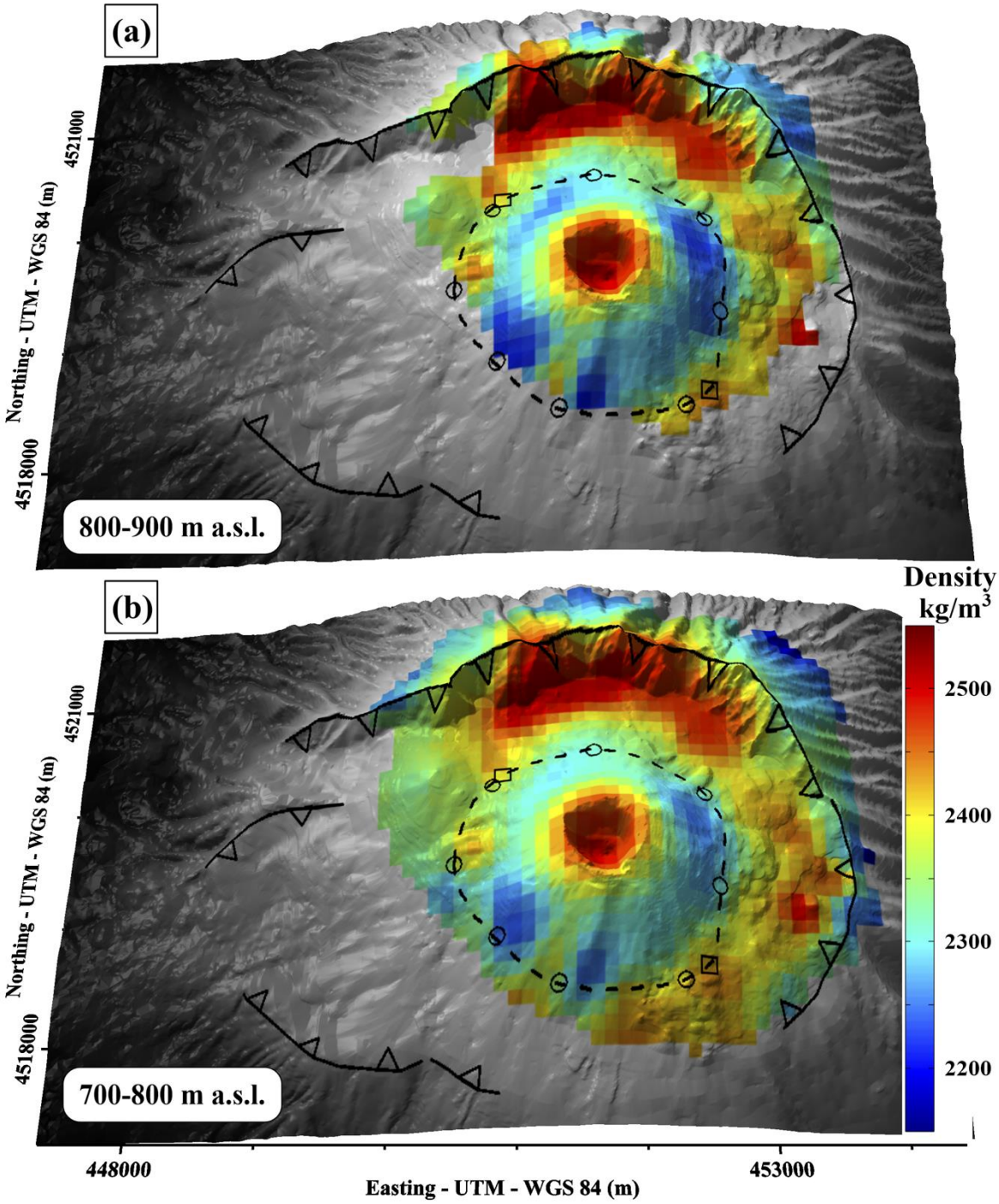

Figure 9: 3-D view of the Somma-Vesuvius displaying the density model and the CO_2 peaks and limit (details in Fig. 7 and Table 2). a) Comparison between the limit defined by the CO_2 peaks with a horizontal density slice between 800 and 900 m a.s.l.; b) The same comparison but for a horizontal density slice between 700 and 800 m a.s.l.. Circles refer to the CO_2 peaks identified along the 8 radial profiles, while squares refer to the NW-SE profile (Poret et al., 2016; see Table 2). Mt. Somma caldera rim is from Cioni et al., 1999.

6. Conclusions

We have carried out 4,018 soil CO_2 measurements along profiles covering the whole Somma-Vesuvius volcanic complex (50 km²) with a measurement spacing of 20 m. The results allowed sub-dividing the studied area in three sectors: 1) the present-day summit area of the Vesuvius cone with the highest CO_2 concentration value (~24,140 ppm) located inside the partially buried 1906 crater rim, 2) the flanks of the Vesuvius cone characterized by weak CO_2 concentrations, and 3) the area located outside Mt. Somma caldera with moderate CO_2 concentrations. This study focuses on the short spatial extension anomalies measured on the flanks of the Vesuvius cone. The CO_2 data revealed a roughly circular degassing structure located between 790 and 975 m a.s.l.. This CO_2 limit was compared with a review of the historical literature available showing similar dimensions of the 1631 caldera boundary (i.e. diameter of ~1,686 m). The quantitative analysis indicates radial discrepancies up to 307 m. The impact of the 1631 caldera on the inner structure of the Vesuvius cone has been also identified by comparing the resulting CO_2 limit with a recent 3-D density model obtained from gravity measurements. This model clearly shows lower density values inside the Vesuvius cone, which suggests a post-1631 filling by volcanic products. This study highlights the importance of carrying out soil CO_2 measurements using a short spacing for identifying weak and local anomalies potentially defining the inner structure of a volcanic edifice. Indeed, by means of 20 m measurement step, this study identified and localized the present-day weak boundary produced by the 1631 caldera. This information is pivotal for monitoring and assessing the volcanic hazards, permitting to identify the potential areas prone to the opening of new eruptive vents.

Acknowledgements

The July 2001 field work was funded by a project of ACI-CATNAT 2001-2003 (L. Jouniaux), and the July 2003 field work by Bourse d'Excellence du Conseil Régional d'Auvergne (AF) and INGV - Osservatorio Vesuviano. The March 2014 field work was funded by MED-SUV Project (European FP7). We are grateful to G. Cairanne, and B. Klein (July 2001), L. Bennati, M. Block, and E. Jacquemin-Guillaume (July 2003) and J. Bernard, E. Brothelande, Y. Fargier and A. Peltier (March 2014) for their help during the field work. We warmly acknowledge M. Leygonie and C. Mezon for the fruitful discussions. The DEM of Vesuvius was kindly provided by G. Vilardo (INGV - Osservatorio Vesuviano). This is IPGP contribution number: 4008.

References

Acocella V., and Funiciello R. (2006). Transverse systems along the extensional Tyrrhenian margin of central Italy and their influence on volcanism. Tectonics 25, TC2003. doi:10.1029/2005TC001845

Acocella V. (2007). Understanding caldera structure and development: An overview of analogue models compared to natural calderas. *Earth-Science Reviews* 85 (3), 125–160

Aiuppa A., Caleca A., Federico C., Gurrieri S., and Valenza M. (2004). Diffuse degassing of carbon dioxide at Somma–Vesuvius volcanic complex (Southern Italy) and its relation with regional tectonics. *J. Volcanol. Geotherm. Res. 133* (1–4), 55–79

Allard P., Hammouya G., and Parello F. (1998). Dégazage magmatique diffus à la Soufrière de Guadeloupe, Antilles. *Comptes Rendus de l'Académie des Sciences-Series IIA-Earth and Planetary Science*, *327*, 5, 315–318

Andronico D., Calderoni G., Cioni R., Sbrana A., Sulpizio R., and Santacroce R. (1995). Geological map of Somma-Vesuvius volcano. *Period Mineral* 64, 77–78

Andronico D., and Cioni R. (2002). Contrasting styles of Mount Vesuvius activity in the period between the Avellino and Pompeii Plinian eruptions, and some implications for assessment of future hazards. *Bull. Volcanol.* 64 (6), 372–391

Anonymous (1631a). Relazione dell'incendio del Vesuvio del 1631. In: L. Riccio, Documenti inediti. Giannini e Figli, Napoli, 1889, pp 513–521

Anonymous (1631b). Lettere, avvisi e notizie diverse sulla eruzione del 1631. In: L. Riccio, Documenti inediti. Giannini e Figli, Napoli, 1889, pp 522–536

Anonymous (1632). Nuovissima relazione dell'incendio successo nel Monte di Somma a 16 dicembre 1631 un'avviso di quello e successo nell'istesso dí nella cittá di Cattaro, nelle parti d'Albania. Egidio Longo, Venezia-Napoli, pp 15

Arnò V., Principe C., Rosi M., Santacroce R., Sbrana A., and Sheridan L.F. (1987). Somma-Vesuvius eruptive history. In: Santacroce, R. (Ed.), Somma-Vesuvius. CNR *Quad. Ric. Sci.* Roma 114, 8, pp 53–103

Arrighi S., Principe C., and Rosi M. (2001). Violent strombolian and subplinian eruptions at Vesuvius during post-1631 activity. *Bull. Volcanol.* 63, 126–150

Barberi F., and Carapezza M.L. (1994). Helium and CO2 soil gas emission from Santorini (Greece). Bull. Volcanol. 56, 335-342Barberi F., Principe C., Rosi M., and Santacroce R. (1995). Scenario eruttivo al Vesuvio 19 nel caso di riattivazione a medio-breve termine. Aggiornamento al 20 gennaio 1995. Rapporto GNV-Protezione Civile, pp 14 (in Italian)

Barberi F., Principe C., Rosi M., and Santacroce R. (1995). Scenario dell'evento eruttivo massimo atteso al Vesuvio in caso di riattivazione a breve-medio termine (Aggiornamento al 20.1.1995), CNR, *Gruppo Nazionale per la Vulcanologia*, Confidential Report to DPC, 19 pp

Barde-Cabusson S., Finizola,A., Revil A., Ricci T., Piscitelli S., Rizzo E., Angeletti B., Balasco M., Bennati L., Byrdina S., Carzaniga N., Crespy A., Di Gangi F., Morin J., Perrone A., Rossi M., Roulleau E., Suski B., and Villeneuve N. (2009). New geological insights and structural control on fluid circulation in La Fossa cone (Vulcano, Aeolian Islands, Italy). *J. Volcanol. Geotherm. Res.* 185, 231–245. doi:10.1016/j.jvolgeores.2009.06.002

Bertagnini A., Landi P., Santacroce R., and Sbrana A. (1991). The 1906 eruption of Vesuvius: from magmatic to phreatomagmatic activity through the flashing of a shallow depth hydrothermal system. *Bull. Volcanol.* 53, 517–532

Bertagnini A., Landi P., Rosi M., and Vigliargio A. (1998). The Pomici di Base plinian eruption of Somma-Vesuvius. *J. Volcanol. Geotherm. Res.* 83 (3), 219–239

Bianco F., Castellano M., Milano G., Ventura G., and Vilardo G. (1998). The Somma-Vesuvius stress field induced by regional tectonics: Evidences from seismological and mesostructural data. *J. Volcanol. Geotherm. Res.* 82, 199–218

Bove V. (1632). Nuove osservazioni fatte sopra gli effetti dell'incendio del Monte Vesuvio. Aggiunte alla decima relazione dello stesso incendio gia' data in luce. Da i 16 di dicembre 1631 fino al 16 di gennaro 1632. *Scoriggio Lazzaro*, Napoli, pp 30

Braccini G.C. (1631). Relazione dell'incendio fattosi nel Vesuvio alli 16 di Dicembre 1631. Scritta dal Signor Abate Giulio Cesare Braccini da Gioviano di Lucca, in una lettera diritta alI'Eminentissimo, e Reverendissimo Signore Card. Girolamo Colonna, per Secondino Roncaglielo, Napoli

Braccini G.C. (1632). Dell'incendio fattosi sul Vesuvio a XVI di Dicembre MDCXXXI e delle sue cause ed effetti. Con la narrazione di quanto è seguito in esso per tutto marzo 1632 e con la storia di tutti gli altri incendi, nel medessimo monte avvenuti. Roncagliolo Secondino, Napoli, pp 104

Brothelande E., Finizola A., Peltier A., Delcher E., Komorowski J.C., Di Gangi F., Borgogno G., Passarella M., Trovato C., and Legendre Y. (2014). Fluid circulation pattern inside La Soufrière volcano (Guadeloupe) inferred from combined electrical resistivity tomography, self-potential, soil temperature and diffuse degassing measurements. *J. Volcanol. Geotherm. Res.* 288, 105–122. doi:10.1016/j.jvolgeores.2014.10.007

Brothelande E., Lénat J.F., Chaput M., Gailler L., Finizola A., Dumont S., Peltier A., Bachèlery P., Barde-Cabusson S., Byrdina S., Menny P., Colonge J., Douillet G., Letort J., Letourneur L., Merle O., Di Gangi F., Nakedau D., and Garaebiti E. (2016). Structure and evolution of

an active resurgent dome evidenced by geophysical investigations: the Yenkahe dome-Yasur volcano system, Vanuatu. *J. Volcanol. Geotherm. Res.* 322, 241–262. doi:10.1016/j.jvolgeores.2015.08.021

Bulifon A. (1694). Esattissima Delineazione del Monte Vesuvio altrimenti detto di Somma, Napoli.

Burnet T. (1699). Telluris Theoria Sacra, Originem et Mutationes Generales Orbis Nostri Accedunt Eiusdem Archaeologiae Philosophicae. Wolters, Amsterdam

Capece A. (1631). Lettere scritte al P. Antonio Capece della Compagnia di Gesù a Roma, 20 e 25 dic. 1631 e 3 genn. 1632. In: L. Riccio, Documenti inediti. Giannini e Figli, Napoli, 1889, pp 495–501

Camarda M., Gurrieri S., and Valenza M. (2006). CO_2 flux measurements in volcanic areas using the dynamic concentration method: Influence of soil permeability. *J. Geophys. Res.: Solid Earth*, 111, B5

Capuano P., Russo G., Civetta L., Orsi G., D'Antonio M., and Moretti R. (2013). The Campi Flegrei caldera structure imaged by 3-D inversion of gravity data. *Geochem. Geophys. Geosyst.*, 14: 4681–4697. doi:10.1002/ggge.20276

Carafa G. (1632). In Opusculum de novassima Vesuvio conflagratione. Epistola Isagogica (IIed). Egidio Longo, Napoli, pp 100

Carapezza M.L., Ricci T., Ranaldi M., and Tarchini L. (2009). Active degassing structures of Stromboli and variations in diffuse CO_2 output related to the volcanic activity. *J. Volcanol. Geotherm. Res.* 182, 3–4, 231–245. doi:10.1016/j.jvolgeores.2008.08.006

Cardellini C., Chiodini G., Frondini F., Granieri D., Lewicki J., and Peruzzi L. (2003). Accumulation chamber measurements of methane fluxes: application to volcanic-geothermal areas and landfills. *Applied Geochem.* 18, 45–54

Carracedo J.C., Principe C., Rosi M., and Soler V. (1993). Time correlation by palaeomagnetism of the 1631 eruption of Mount Vesuvius. Volcanological and volcanic hazard implications. *J. Volcanol. Geotherm. Res.* 58, 1–4, 203–209. doi:10.1016/0377-0273(93)90108-4

Chiodini G., Cioni R., Guidi M., Raco B., and Marini L. (1998). Soil CO_2 flux measurements in volcanic and geothermal areas. *Applied Geochem.* 13, 5, 543–552

Chiodini G., Frondini F., Cardellini C., Granieri D., Marini L., and Ventura G. (2001a). CO_2 degassing and energy release at Solfatara volcano, Campi Flegrei, Italy. *J. Geophys. Res.* 106, 16213–16221. doi:10.1029/2001JB000246

Chiodini G., Marini L., and Russo M. (2001b). Geochemical evidence for the existence of High-temperature hydrothermal brines at Vesuvius volcano, Italy. *Geochemica et Cosmochimica Acta* 65, 13, 2129–2147

Cioni R., Santacroce R., and Sbrana A. (1999). Pyroclastic deposit as a guide for reconstructing the multi-stage evolution of the Somma-Vesuvius caldera. *Bull. Vulcanol.* 60, 207–222

Cioni R., Bertagnini A., Santacroce R., and Andronico D. (2008). Explosive activity and eruption scenarios at Somma-Vesuvius (Italy): Towards a new classification scheme. *J. Volcanol.Geotherm. Res.* 178, 331–346. doi:10.1016/j.jvolgeores.2008.04.024

Del Pezzo E., Chiodini G., Caliro S., Bianco F., and Avino R. (2013). New insights into Mt. Vesuvius hydrothermal system and its dynamic based on a critical review of seismic tomography and geochemical features. *Annals of Geophys.* 56, 4, S0444. doi:10.4401/ag-6450

DPC (1995). Pianificazione Nazionale d'Emergenza dell'Area Vesuviana. Dipartimento della Protezione Civile, Roma

DPC (2015). Dossier: Update of the National Emergency Plan for Vesuvius. Dipartimento della Protezione Civile, Roma. (http://www.protezionecivile.gov.it/jcms/en/view_dossier.wp?contentId=DOS37087)

Drummond J. (1845). Letters from James, Earl of Perth, Lord Chancellor of Scotland, etc. to his sister, the Countess of Errol, and other members of his family, London

Etiope G., Beneduce P., Calcara M., Favali P., Frugoni F., Schiattarella M., and Smriglio G. (1999). Structural pattern and CO_2–CH_4 degassing of Ustica Island, Southern Tyrrhenian basin. *J. Volcanol. Geotherm. Res.* 88, 291–304

Evelyn J. (1644). The diary of John Evelyn a C. G. Capuano, in Viaggiatori britannici a Napoli tra ‘500 e ‘600, Pietro Laveglia Editore, 1994, Salerno

Farrar C.D., Sorey M.L., Evans W.C., Howle J.F., Kerr B.D., Kennedy B.M., King C.Y., and Southon J.R. (1995). Forest-killing diffuse CO_2 emission at Mammoth Mountain as a sign of magmatic unrest. *Nature* 376, 675–678. doi:10.1038/376675a0

Finizola A., Sortino F., Lénat J.F., Valenza M. (2002). Fluid circulation at Stromboli volcano (Aeolian Islands, Italy) from self-potential and soil gas surveys. *J. Volcanol. Geotherm. Res.* 116, 1–2, 1–18

Finizola A., Sortino F., Lénat J.F., Aubert M., Ripepe M., and Valenza M. (2003). The summit hydrothermal system of Stromboli: new insights from self-potential, temperature, CO_2 and fumarolic fluids measurements, with structural and monitoring implications. *Bull. Volcanol.* 65, 486–504. doi:10.1007/s00445-003-0276-2

Finizola A., Lénat J.F., Macedo O., Ramos D., Thouret J-C., and Sortino F. (2004). Fluid circulation and structural discontinuities inside Misti volcano (Peru) inferred from self-potential measurements. *J. Volcanol. Geotherm. Res.* 135, 4, 343–360. doi:10.1016/j.jvolgeores.2004.03.009

Finizola A., Revil A., Rizzo E., Piscitelli S., Ricci T., Morin J., Angeletti B., Mocochain L., and Sortino F. (2006). Hydrogeological insights at Stromboli volcano (Italy) from geoelectrical, temperature, and CO_2 soil degassing investigations. *Geophys. Res. Lett.* 33, L17304. doi:10.1029/2006GL026842

Finizola A., Aubert M., Revil A., Schütze C., and Sortino F. (2009). Importance of structural history in the summit area of Stromboli during the 2002–2003 eruptive crisis inferred from temperature, soil CO_2, self-potential, and electrical resistivity tomography. *J. Volcanol. Geotherm. Res.* 183, 213–227. doi:10.1016/j.jvolgeores.2009.04.002

Finizola A., Ricci T., Deiana R., Barde-Cabusson S., Rossi M., Praticelli N., Giocoli A., Romano G., Delcher E., Suski B., Revil A., Menny P., Di Gangi F., Letort J., Peltier A., Villasante-Marcos V., Douillet G., Avard G., Lelli M. (2010). Adventive hydrothermal circulation on Stromboli volcano (Aeolian Islands, Italy) revealed by geophysical and geochemical approaches: Implications for general fluid flow models on volcanoes. *J. Volcanol. Geotherm. Res.*, 196, 111-119. doi:10.1016/j.jvolgeores.2010.07.022.

Froger J.L., Lénat J.F., Chorowicz J., Le Pennec J.L., Bourdier J.L., Kose O., Zimitoğlu O., Gundogdu N., and Gourgaud A. (1998). Hidden calderas evidenced by multisource geophysical data; example of Cappadocian Calderas, Central Anatolia. *J. Volcanol. Geotherm. Res.* 85, 1, 99–128. doi:10.1016/S0377-0273(98)00052-3.

Frondini F., Chiodini G., Caliro S., Cardellini C., Granieri D., and Ventura G. (2004). Diffuse CO_2 degassing at Vesuvio, Italy. *Bull. Volcanol.* 66, 642–651

Gerlach T.M., (1986). Exsolution of H_2O, CO_2, and S during eruptive episodes at Kilauea Volcano, Hawaii, *J. Geophys. Res.: Solid Earth*, 91–B12, 12,177–12,185

Giuliani G. (1632). Trattato del Monte Vesuvio e de' suoi incendi. Egidio Longo, Napoli. pp 254

Granieri D., Carapezza M.L., Chiodini G., Avino R., Caliro S., Ranaldi M., Ricci T., and Tarchini L. (2006). Correlated increase in CO_2 fumarolic content and diffuse emission from La Fossa crater (Vulcano, Italy): Evidence of volcanic unrest or increasing gas release from a stationary deep magma body? *Geophys. Res. Lett.* 33, L13316. doi:10.1029/2006GL026460

Granieri D., Carapezza M.L., Avino R., Caliro S., Cardellini C., Chiodini G., Donnini M., Minopoli C., Ranaldi M., Ricci T., and Tarchini L. (2013). Level of carbon dioxide diffuse

degassing from the ground of Vesuvio: comparison between extensive surveys and inferences on the gas source. *Annals of Geophys.* 56, 4, S0449. doi:10.4401/ag-6455

Guidoboni E. (2008). Vesuvius: A historical approach to the 1631 eruption "cold data" from the analysis of three contemporary treatises. *J. Volcanol. Geotherm. Res.* 178, 347–358. doi:10.1016/j.jvolgeores.2008.09.020

Ippolito F., Ortolani F., and Russo M. (1973). Struttura marginale tirrenica dell'Appennino Campano: Reinterpretazione dei dati di antiche ricerche di idrocarburi. *Mem. Soc. Geol.* Italy. 12, 227–250

Lewicki J.L., Connor C., St-Amand K., Stix J., and Spinner W. (2003). Self-potential, soil CO_2 flux, and temperature on Masaya volcano, Nicaragua. *Geophys. Res. Lett.* 30, 15, 1–4. doi:10.1029/2003GL017731 1817

Linde N., Ricci T., Baron L., Shakas A., and Berrino G. (2017). The 3-D structure of the Somma-Vesuvius volcanic complex (Italy) inferred from new and historic gravimetric data. *Scientific Reports* 7, 8434. doi:10.1038/s41598-017-07496-y

Magalotti L. Conte (1779). Lettera al Sig. Vincenzo Viviani, in cui si descrive il Vesuvio nel 1663, in: Anonimous, Dei Vulcano o Monti ignivomi, T. II pp II

Marianelli P., Metrich N., and Sbrana A. (1999). Shallow and deep reservoirs involved in magma supply of the 1944 eruption of Vesuvius. *Bull. Volcanol.* 61, 48–63

Marinoni L. (1995). The Monte Somma scarp: new preliminary stratigraphy and structural insights. *Per. Mineral.* 64, 219–221

Masculo G.B. (1633). De incendio Vesuvii excitato XVlI kal Ianuarii anno trigesimo primo saeculi decimiseptimi, Roncaglido, Napoli

Masino di Calvello A.M. (1632). Distinta relazione dell'incendio del sevo Vesuvio alli 16 di dicembre 1631 successo. Con la relatione del incendio della citta, di Pozzuoli e cause de' terremoti al tempo di Don Pietro de Toleto Vicere' in questo regno nell'anno 1534. Roncagliolo Domenico, Napoli, pp 36

Mastrolorenzo G., Munno R., and Rolandi G. (1993). Vesuvius 1906: a case study of a paroxysmal eruption and its relation to eruption cycles. *J. Volcanol Geotherm. Res.* 58, 1–4, 217–237. doi:10.1016/0377-0273(93)90110-D

Mastrolorenzo G., Palladino D. M., Vecchio G., and Taddeucci J. (2002). The 472 AD Pollena eruption of Somma-Vesuvius (Italy) and its environmental impact at the end of the Roman Empire. *J. Volcanol Geotherm. Res.* 113, 1, 19–36. doi:10.1016/S0377-0273(01)000248-7

Mauri G., Williams-Jones G., and Saracco G. (2012). A geochemical and geophysical investigation of the hydrothermal complex of Masaya volcano, Nicaragua. *J. Volcanol. Geotherm. Res.*, vol.227-228, p. 15-31, doi:10.1016/j.jvolgeores.2012.02.003

Merle O., and Lénat J.F. (2003). Hybrid collapse mechanism at Piton de la Fournaise volcano, Reunion Island, Indian Ocean. *J. Geophys. Res.: Solid Earth*. doi:10.1029/2002JB002014

Mielnick P.C., and Dugas W.A. (2000). Soil CO_2 flux in a tallgrass prairie. Soil Biology & Biochem. 32, 221–228

Nazzaro A. (1989). L'eruzione del 1631 ed il collasso del Vesuvio in base all'analisi delle fonti contemporanee. *Rend. Soc. Ital. Mineral. Petrol.* 43, 725–732

Orsi G., Civetta L., Del Gaudio C., de Vita S., Di Vito M.A., Isaia R., Petrazzuoli S.M., Ricciardi G., and Ricco C. (1999). Short-term ground deformations and seismicity in the nested Campi Flegrei caldera (Italy): an example of active block-resurgence in a densely populated area. *J. Volcanol. Geotherm. Res.*, 91, 2–4, 415–451

Perret F.A. (1924). The Vesuvius eruption of 1906. Study of a volcanic cycle. *Carnegie Inst Washington Pub* 339, pp 151

Pescatore T.S., and Sgrosso I. (1973). I rapporti tra la piattaforma campano-lucana e la piattaforma abruzzese-campana nel casertano. *Boll. Soc. Geol. Italy.* 92, 925–938

Poret M., Ricci T., Finizola A., Delcher E., Peltier A., Antoine R., Bernard J., Boudoire G., Brothelande E., Fanizza G., Fargier Y., Gailler L., Gueguen E., Gusset R., Matera A., Mezon C., Piscitelli S., Portal A., Rizzo E., Rossi M., Calamita G., Bellucci Sessa E., and Nave R. (2016). Multidisciplinary investigation (ERT, CO_2, SP, and T) reveals fluid circulation at Somma-Vesuvius. *EGU General Assembly*, Vienna, 17–22 April 2016, Poster

Principe C., Brocchini D., Arrighi S., Luongo G., Giordano D., Perillo M., Di Muro A., Martì J.M., Bisson M., and Paolillo A. (2010). Vesuvius volcano-tectonic history: a new perspective. Collapse Caldera Workshop 2010, "Dynamics of caldera: collapse and unrest". October 3–9, 2010, La Réunion Island

Raymond J. (1648): An Itinerari Contayning a Voyage Made through Italy, London

Revil A., Finizola A., Sortino F., and Ripepe M. (2004). Geophysical investigations at Stromboli volcano, Italy. Implications for ground water flow and paroxysmal activity. *Geophys. J. Int.*, 157, 426–440. doi:10.1111/j.1365-246X.2004.02181.x

Revil A., Finizola A., Piscitelli S., Rizzo E., Ricci T., Crespy A., Angeletti B., Balasco M., Barde Cabusson S., Bennati L., A. Bolève., Byrdina S., Carzaniga N., Di Gangi F., Morin J., Perrone A., Rossi M., Roulleau E., and Suski B. (2008). Inner structure of La Fossa di Vulcano (Vulcano Island, southern Tyrrhenian Sea, Italy) revealed by high resolution electric resistivity tomography coupled with self-potential, temperature, and CO_2 diffuse degassing measurements. *J. Geophys. Res.*, 113, B07207. doi:10.1029/2007JB005394

Revil A., Finizola A., Ricci T., Delcher E., Peltier A., Barde-Cabusson S., Avard G., Bailly T., Bennati L., Byrdina S., Colonge J., Di Gangi F., Douillet G., Lupi M., Letort J., and Tsang

Hin Sun E. (2011). Hydrogeology of Stromboli volcano, Aeolian Islands (Italy) from the interpretation of resistivity tomograms, self-potential, soil temperature, and soil CO_2 concentration measurements. *Geophys. J. Int.*, 186, 1078-1094. doi:10.1111/j.1365-246X.2011.05112.x

Ricci T., Nave R., and Barberi F. (2013). Vesuvio civil protection exercise MESIMEX: survey on volcanic risk perception. *Annals of Geophys.* 56, 4, S0452.

Ricci T., Finizola A., Poret M., Delcher E., Peltier A., Antoine R., Linde N., Revil A., Bernard J., Brothelande E., Fanizza G., Fargier Y., Gailler L., Gueguen, E. Gusset R., Matera A., Mezon C., Piscitelli S., Portal A., Rizzo E., Rossi M., Baron L., Shakas A., Boudoire G., Calamita G., Gaudin D., Sciarra A., Tournigand P.Y. Inner structure and hydrothermal circulation at Somma Vesuvius volcanic complex (Italy) inferred by high-resolution electrical resistivity tomography, gravity, self-potential, temperature, and soil degassing measurements. *J. Volcanol. Geotherm. Res.* In prep.

Rocco A. (1632). Oratione devotissima alla gloriosa Vergine Maria dell'Arco (e descrizione dell'incendio del Monte Vesuvio avvenuto in dicembre 1631). Sant'Anastasia, Napoli, pp 36

Roche O., Druitt TH., and Merle O. (2000). Experimental study of caldera formation. *J. Geophys. Res.: Solid Earth* 105 (B1), 395–416

Rolandi G., Munno R., and Postiglione I. (2004). The AD 472 eruption of the Somma volcano. *J. Volcanol. Geotherm. Res.* 129, 4, 291–319

Rosi M., and Santacroce R. (1983). The AD 472 "Pollena" eruption: volcanological and petrological data for this poorly-known, Plinian-type event at Vesuvius. *J. Volcanol. Geotherm. Res.* 17, 1, 249–271

Rosi M., Principe C., and Vecci R. (1993). The 1631 eruption of Vesuvius reconstructed from the review of chronicles and study of deposits. *J. Volcanol. Geotherm. Res.* 58, 151–182

Santacroce R. (1987). Somma-Vesuvius. *Quaderni. Ric. Sci.* 114, pp 230, Cons. Naz. delle Ric., Rome

Santacroce R., Bertagnini A., Civetta L., Landi P., and Sbrana A. (1993). Eruptive dynamics and petrogenetic processes in a very shallow magma reservoir. *J. Petrol.* 34, 383–425

Santacroce R., and Sbrana A. (2003). Geological map of Vesuvius at the scale 1:15,000. SELCA editore, Firenze

Santactoce R., Cioni R., Marianelli P., Sbrana A., Sulpizio R., Zanchetta G., Donahue D.J., and Joron, J.L. (2008). Age and whole rock-glass compositions of proximal pyroclastics from the major explosive eruptions of Somma-Vesuvius: A review as a tool for distal

tephrostratigraphy. *J. Volcanol. Geotherm. Res.* 177, 1–18. doi:10.1016/j.jvolgeores.2008.06.009

Schütze C., Vienken T., Werban U., Dietrich P., Finizola A., and Leven C. (2012). Joint application of geophysical methods and Direct Push-soil gas surveys for the improved delineation of buried fault zones. J. Appl. Geophys. 82, 129-136, doi: 10.1016/j.jappgeo.2012.03.002.

Sinclair A.J. (1974). Selection of threshold values in geochemical data using probability graphs. *J. Geochem. Explor.* 3, 2, 129–149

Sorrentino I. (1734). Istoria del Monte Vesuvio. Divisata in due libri. Severini Giuseppe, Napoli, pp 231

Sulpizio R., Mele D., Dellino P., and La Volpe L. (2005). A complex, Subplinian-type eruption from low-viscosity, phonolitic to tephri-phonolitic magma: the AD 472 (Pollena) eruption of Somma-Vesuvius, Italy. *Bull. Volcanol.* 67 (8), 743–767

Tadini A., Bisson, M., Neri A., Cioni R., Bevilacqua A., and Aspinall W.P. (2017). Assessing future vent opening locations at the Somma-Vesuvio volcanic complex: 1. A new information geodatabase with uncertainty characterizations. *J. Geophys. Res.: Solid Earth*, 122, 4336–4356. doi:10.1002/2016JB013858

Ventura G., Vilardo G., and Bruno P.P. (1999). The role of flank collapse in modifying the shallow plumbing system of volcanoes: an example from Somma-Vesuvius, Italy. *Geophys. Res. Lett.* 26, 3681–3684

Ventura G., and Vilardo G. (2006). Tomomorphometry of the Somma-Vesuvius volcano (Italy). *Geophys. Res. Lett.* 33, L17305. doi:10.1029/2006GL027116

Vilardo G., Bronzino G., Alessio G., Bellucci Sessa E., and Nappi R. (2008). GeoDATA Finder: Sistema di consultazione on-line della banca dati territoriali del Laboratorio di Geomatica e Cartografia, Istituto Nazionale di Geofisica e Vulcanologia, Sezione di Napoli Osservatorio Vesuviano; http://ipf.ov.ingv.it/dbnas/login_user.asp

Viveiros F., Cardellini C., Ferreira T., Caliro S., Chiodini G., and Silva C. (2010). Soil CO_2 emissions at Furnas volcano, São Miguel Island, Azores archipelago: Volcano monitoring perspectives, geomorphologic studies, and land use planning application. *J. Geophys. Res.* 115, B12208. doi:10.1029/2010JB007555

Williams-Jones G., Stix J., Heiligmann M., Charland A., Sherwood Lollar B., Arner N., Garzon G., Barquero J., and Fernandez E., 2000. A model of diffuse degassing at three subduction-related volcanoes. *Bull. Volcanol.* 62, 130–142

Highlights

1 More than 4000 soil CO_2 measurements over the Somma-Vesuvius volcanic edifice (>50 km^2).

2 Production of the soil CO_2 concentration map over the domain at very high spatial resolution (40 m).

3 Benefiting of the 20-m step measurement for identifying the main structural elements.

4 Local CO_2 maxima on each radial profile lead to characterize a circular boundary coinciding with the caldera produced by the 1631 sub-Plinian eruption.